Fuzzy C-means Clustering For Retinal Layer Segmentation On High Resolution OCT Images

Markus A. Mayer[1,2] , Ralf P. Tornow[3], Joachim Hornegger[1], Friedrich E. Kruse[3]
[1] Chair of Pattern Recognition,
[2] Graduate School in Advanced Optical Technologies (SAOT),
[3] Department of Ophthalmology
University of Erlangen-Nuremberg, Erlangen, Germany
markus.mayer@informatik.uni-erlangen.de

Spectral domain optical tomography allows the aquisition of high-resolution images of the retina depth profile. The thickness of these layers can be an indicator for a glaucoma diagnosis. We propose a novel algorithm to segment the nerve fiber layer on circular B-Scans around the optic disc and to obtain geometry corrected images . Feature vectors are calculated for the extrema along the smoothed derivative of all A-Scans. These feature vectors are automatically clustered with fuzzy C-means clustering. The assumption is made that the resulting clusters correspond to the different retinal layer borders. On the upper nerve fiber layer 98% and on the lower nerve fiber layer 72 % of the border points are detected within a 2 pixel range of a manual segmentation carried out by the authors on 12 B-Scans from both normal and glaucoma patients.

1 Introduction

The benefits of optical coherence tomography (OCT) [1] for ophthalmology have become more and more obvious in the recent years. Spectral domain OCT systems make it possible to obtain in-vivo images of the retina, showing a high resolution depth profile of the retinal layers [2]. The thickness of the these layers, especially the nerve fiber layer (NFL), are reliable indicators for a glaucoma diagnosis [3, 4].

To assist ophthalmologists, automated methods that extract glaucoma indicators from images and present them in a clinically comprehensible way are being developed [5]. In the field of OCT imaging early automated methods segmented the complete retina [6] on time domain OCT images. Today different methods are published ranging from complete retina segmentation in 3D [7], automated NFL segmentation on consecutive frames in an OCT movie [8] or segmenting all retinal layers using a half-automated system [9]. The drawback of all these methods is that either no results for glaucoma patients are shown [7, 8] or the method fails on glaucoma patients due to preassumptions made on the layer shapes and thus needs a parameter adaption [9]. Furthermore, all methods make use of computationally intensive anisotropic diffusion methods for preprocessing, i.e. denoising and contrast enhancement.

We present a fast nerve fiber layer segmentation method that is applicable on normal and glaucoma patients without parameter adaption. During the segmentation process an image with corrected geometry is generated.

2 Data

To clarify denotations, an A-Scan is one line depth profile at a specific point, while a B-Scan denotes a 2D depth profile consisting of several A-Scans. Circular B-scans (diameter 3.4mm, 512 or 768 A-scans) around the optic disc were acquired using a Spectralis HRA+OCT (Heidelberg Engineering) (see Fig. 1). The depth resolution of the OCT is 7 µm in tissue. One A-Scan consists of 496 pixels with a height of 3,87µm each. This results in OCT images of 512x496 or 768x496 pixels. The columns correspond to the individual A-Scans. The different A-Scans are determined by the x-coordinate of the image coordinate

system, the position in the A-Scan by the y-coordinate.

The anterior NFL boundary is the top-most retinal layer boundary on the OCT image. It will be denoted upper NFL boundary (UNFL) in the following, due to its location in the OCT image. Analogously, the posterior NFL boundary will be denoted lower NFL boundary (LNFL). The retinal pigment epithel (RPE) is the bottom-most visible retinal layer on the OCT images.

For the evaluation of our algorithm B-scans of 5 normal and 7 glaucomatous eyes were used. For these data sets a manual segmentation carried out by the authors defines the gold standard for the evaluation. Manual segmentations of unexperienced persons were also available.

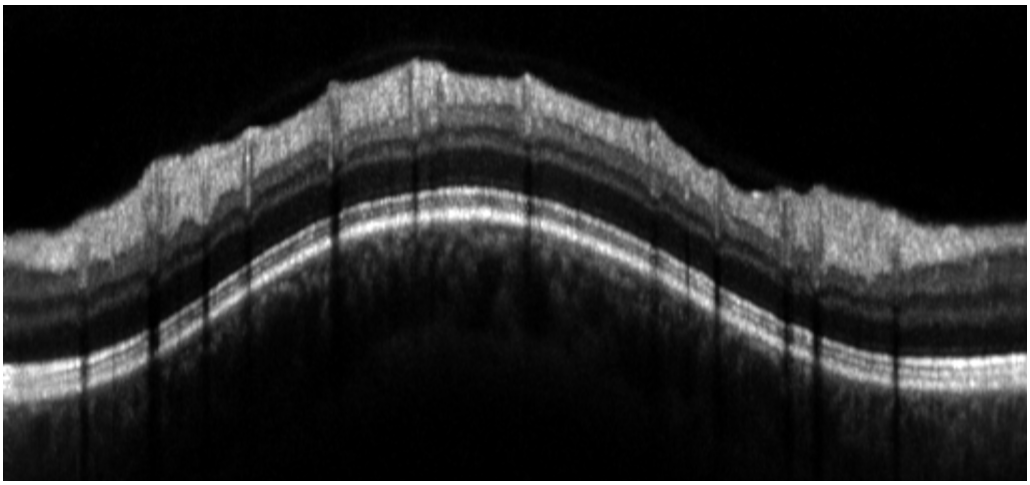

a)

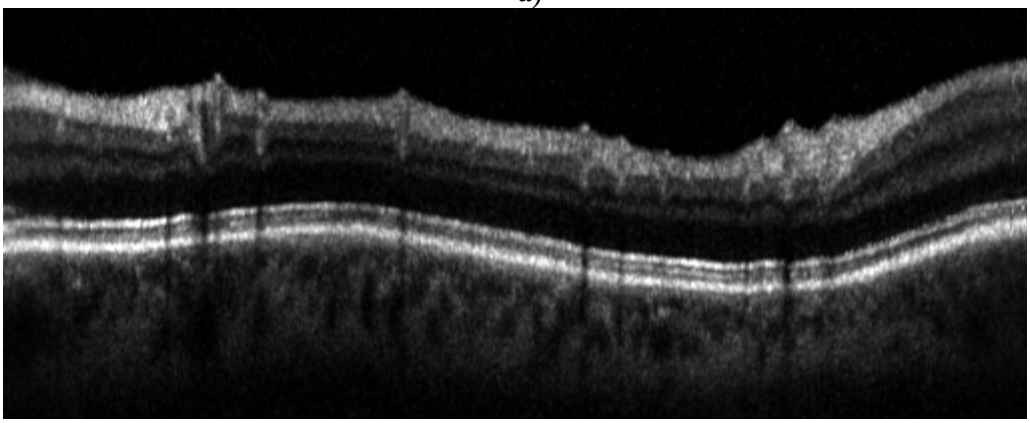

b)

Fig 1. Circular OCT B-Scan examples. Bias is removed and intensities are normalized. Selection out of a 512x496 image. a) Normal eye. b) Glaucomatous eye

3 Method

The main idea of the algorithm is that only pixels that most likely lie on a retina layer border are taken into account for the segmentation. The extrema along the Gaussian smoothed first derivative of the A-Scans are taken as candidates and are automatically assigned to the different retinal layer borders. Because the state of health and shapes of the scanned eyes differ strongly, it was decided that no prior knowledge should be provided to the algorithm. Instead, the assignment is carried out by an unsupervised automated clustering. The steps of the algorithm are explained in detail in the following:

1. **Preprocessing**
   First, the noise bias of the OCT image is removed. The intensity values of the 10 upper- and lowermost lines in the OCT image, which show only show dark and noisy background, are sorted. The average of the top third pixels with highest intensity values is computed and subtracted from the OCT image. Second, intensity outliers are eliminated. All pixels on the image are sorted according to intensity values, and the 0.05% highest values are set to the lowest value within their range. The normalisation parameters mentioned in this step showed to result in a contrasty image without structure loss and were determined by test runs on the available data. After that, all intensity values of image are rescaled to [0, 1] (see Fig. 2b).
2. **Extrema Detection**
   The gradient along the columns of the OCT image (A-Scans) is computed with central differences and smoothed by a 1D Gaussian filter with a standard deviation of $\sigma = 3$. The extrema with the highest absolute values are identified by a search along the lines. Test runs on the data sets have shown that keeping the 6 highest extrema for further computation provides good results.
3. **Feature Vector Calculation**
   For each extremum a feature vector is calculated. Used features are: Position in the A-Scan, intensity values in a 2 pixel neighbourhood above and below in the A-Scan and gradient, intensity values in a 2 pixel neighbourhood above and below in a by a factor of 3 downscaled version of the A-Scan and gradient, intensity sums above and below in the A-Scan, intensity sums in a neighbourhood of 3 pixels in the B-Scan, number of extrema in a 5 pixel neighbourhood in the B-Scan. The features used and their number depends on the expected clustering result and number of clusters in step 4. The given values correspond to the parameters given in step 4. The single features are normalized to the range of [-1,1] along all extrema.
4. **Clustering**
   The assumption is made, that by clustering the feature vectors automatically, the resulting clusters are representatives of the different layer borders. Results show that this assumption holds roughly for the above mentioned feature choice. For an automated clustering, fuzzy C-means was chosen. No additional information was given to the clustering algorithm. Six different clusters were generated (see Fig. 2c). A direct relationship of the clusters to retinal layer borders is not always the case, as there may appear clusters consisting of noise, or two retinal layer borders share one cluster (see Fig. 2c).
5. **Geometry Correction**
   In this step, a retinal layer border is identified that can be taken as a baseline to flatten the B-Scan. Possible layers are: Retinal pigment epithel, outer photoreceptor segment or the lower border of the inner photoreceptor segment. A polynomial of degree 5 is fitted to the 3 clusters with the lowest mean y-coordinate of the extrema, and the cluster which best matches the fitting polynomial is taken. This cluster is smoothed and formed to a continuous border by interpolating holes, removing outliers (see step 6), median filtering with a window of 9 and Gaussian filtering with a standard deviation of 3. In the following, this border is denoted as baseline. The A-Scans are realigned such that the baseline is flat, i.e. all y-coordinates of the border have the same value in the resulting image (see Fig. 2d).
   Optionally, steps 3 and 4 can be repeated on the geometry-corrected version of the OCT image. As test runs on the data sets have shown, this improves the results. The goal after geometry correction is to segment the NFL, so only extrema above the baseline have to be taken into account. The 5 highest extrema of the derivative per A-Scan clustered into 4 classes yield good results (see Fig 2e). Additional processing time for the repetition is much lower than the original steps, because the image size is

reduced significantly due to the geometry correction and less extrema are clustered.

6. **Identification of the nerve fiber layer**
   The cluster corresponding to the UNFL is usually the top-most cluster on the image. It may be that a cluster consisting of noise extrema lies above, but this case is easily identified by the high variations along the y-coordinates of these extrema. Test runs have shown that a combination of a the first extrema below the UNFL and the cluster below the UNFL cluster yield a good initial LNFL segmentation.

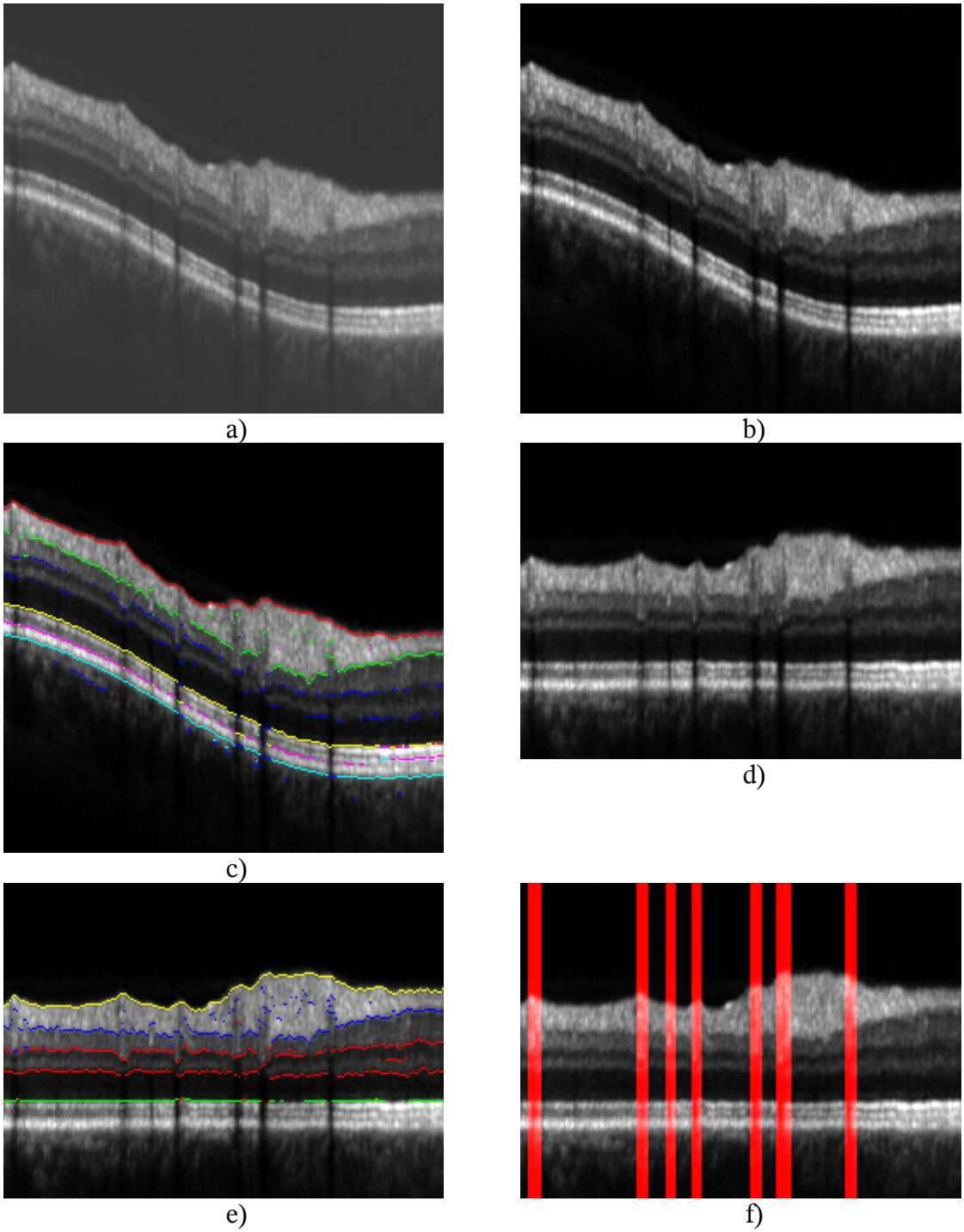

Fig 2. Processing steps. Images are selections out of a 512x496 OCT B-Scan (see Fig. 1)
a) Original OCT B-Scan image. b) Removed Bias and normalized intensity values
c) Extrema after clustering into 6 classes d) geometry-corrected image
e) Extrema detection and clustering into 4 classes f) Marked blood vessel regions

The LNFL segmentation is improved by marking the extrema in blood vessel regions as invalid. Blood vessels prevent the laser light of the OCT system from penetrating deeper into the retina tissue which leads to vertical shadows in the B-Scans that cause false segmentation results. These shadow regions are identified by calculating the mean intensity values in a 5 pixel area around the baseline. Those A-Scans, where the sum of the 5 pixel intensities near the baseline are below half of the mean, are marked as blood vessel regions. These marked regions are expanded by 2 A-Scans on each side (see Fig. 2f).

The UNFL and LNFL clusters are then transformed to continuous lines. First, outliers are eliminated. These are line segments shorter than 5 consecutive points and extrema that are distant from a polynomial of degree 5 fitted to the cluster points. Then, gaps and invalid regions are linearly interpolated. Median filtering with a window of 7 and Gaussian smoothing with a standard deviation of $\sigma = 1$ yield the final NFL borders (see Fig. 3).

4 Evaluation

To evaluate the proposed algorithm, a manual segmentation was carried out by the authors on the data sets from 5 normal and 7 glaucoma eyes using a Matlab (The MathWorks, Inc.) GUI. Considering the fact that small local errors and small offsets along complete lines are negligible for a clinically usable segmentation result, a segmented border point was taken as correct if it lay in a 2 pixel range from the manual segmentation. Using this evaluation method, 98% of the UNFL points and 72% of the LNFL points on all data sets were segmented correctly.

The geometry correction failed on 2 of the 12 data sets. This failure had no impact on the segmentation of the NFL.

Computation time is 40s on a 2Ghz Pentium IV for a 512x496 circular B-scan using a Matlab implementation.

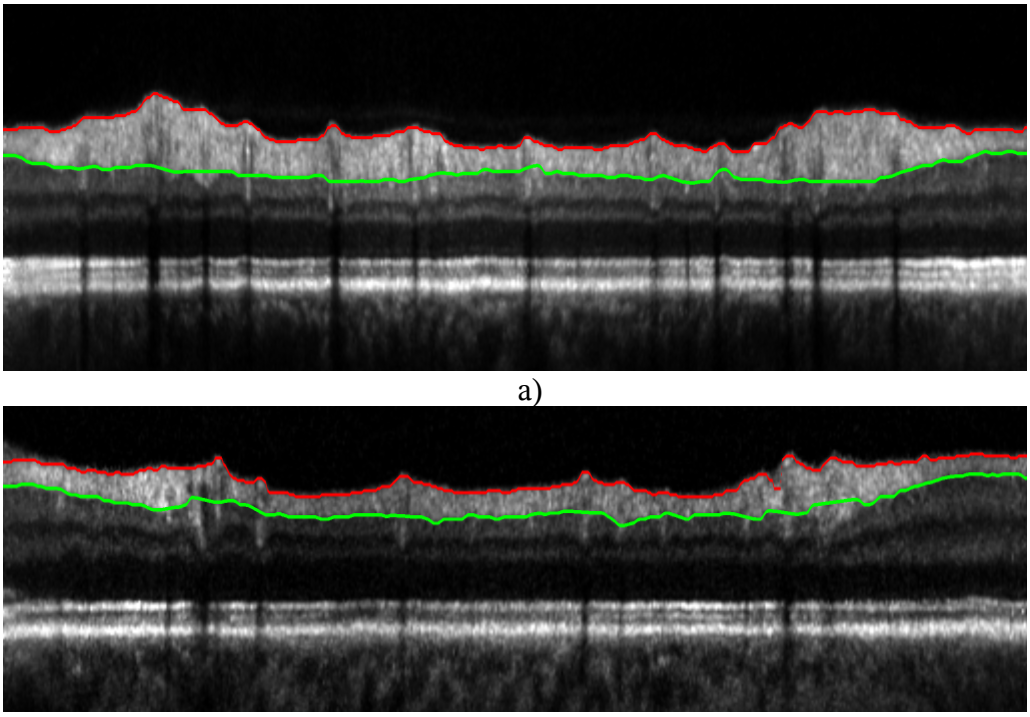

a)

b)

Fig 3. Nerve fiber layer segmentation results a) Normal eye b) Glaucomatous eye

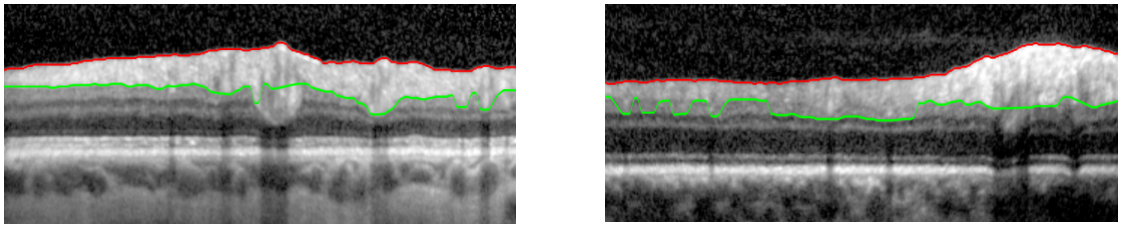

a) b)

Fig 4. Failures of the lower nerve fiber layer border segmenation. a) Interpolation over blood vessel region b) Lack of contrast on boundary

5 Discussion

The method detects the upper NFL boundary reliably, as constituted by the presented high accuracy. The automated method fails on the lower NFL boundary because of either interpolation issues in large blood vessel regions (see Fig. 4a) or lack of contrast on the lower NFL boundary (see Fig. 4b). Such lack of contrast and thus missing information on the location of the lower NFL boundary will most likely lead to a failure of any automated method without further prior knowledge. Comparing manual segmentations from people working in the field of ophthalmology and others has shown that without prior knowledge humans produce similar errors. An automated segmentation that allows manual interaction supervised by an ophthalmologist may be the solution to deliver exact indicator values, i.e. the NFL thickness, for glaucoma diagnosis.

The geometry correction has two advantages: Scan-dependent geometry distortions in the B-Scan happen due to differing distances of the OCT system to the retina as well as distortions due to slight movements of the eye during the inspection. Each A-Scan is taken individually, so neighbourhood information doesn't necessarily reflect real geometry. The correction leads to an improved comparability between subjects and between inspections carried out at different dates. Furthermore, 2D image processing as for example median filtering can be carried out on valid neighbourhood information which reduces artefacts 2D processing may generate on uncorrected B-Scans [10].

6 Outlook

We presented results for a segmentation of the NFL and geometry correction on circular B-Scans. Because a NFL thickness map generated out of a volume consisting of several line B-Scans has advantages in terms of longitudinal and local registration issues over the circular B-Scan [8], an extension to 3D Data is currently in work. A modification of the algorithm for the segmentation of all retinal layers has to be evaluated.

7 Conclusion

We presented a fast retinal layer segmentation method on high resolution OCT scans. It is based on the assumption that an unsupervised clustering of feature vectors calculated for probable retinal layer points yields to a separation of the points into different retinal layer border classes. The method is applicable to normal as well as pathological data, different patients and varying scanner settings without parameter adaption. An ophthalmologist can be assisted in his diagnosis by this new objective and reproducible measurement of the NFL thickness. In addition a visually more informative, geometry-corrected image is generated during the same process.

Acknowledgement

This work has been supported by the Erlangen Graduate School of Advanced Optical Technologies.

References

[1] D. Huang, E.A. Swanson et al.: Optical Coherence Tomography. Science, Nov. 1991: Vol.254(5035), 1178-81, 1991

[2] M. Wojtkowski, R. Leitgeb et al.: In vivo human retinal imaging by Fourier domain optical coherence tomography. Journal of Biomedical Optics, Vol 7(3), 457-463, July 2002

[3] A. Aydin, G. Wollstein et al.: Optical Coherence Tomography Assesment of Retinal Nerve Fiber Layer Thickness Changes after Glaucoma Surgery. Ophtalmology, Vol. 110(8), 1506-1511, Aug. 2003

[4] V. Guedes, J. Schuman et al.: Optical Coherence Tomography Measurement of Macular and Nerve Fiber Layer Thickness in Normal and Glaucomatous Eyes. Ophtalmology, Vol. 110(1), 177-189, Jan. 2003

[5] R. Bock, J. Meier et al.: Classifying glaucoma with image-based features from fundus photographs. Lecture Notes in Computer Science (LNCS) 4713 (DAGM Heidelberg 2007), Vol. 4713/2007, 355-365, Sept. 2007

[6] D. Koozekanani, K. Boyer, et al.: Retinal Thickness Measurements From Optical Coherence Tomography Using a Markov Boundary Model. IEEE Transactions on Medical Imaging, Vol 20(9), 900-916, Sept. 2001

[7] M. Haeker, M. Abramoff et al.: Segmentation of the Surface of the Retinal Layer from OCT Images. MICCAI 2006, 800-807, Sept. 2006

[8] M. Mujat, R.C. Chan, et al.: Retinal nerve fiber layer thickness map determined from optical coherence tomography images. Optics Express Vol. 13(23), 9480-9491, Nov. 2005

[9] D.A. Fernandez, H.M. Salinas, et al.: Automated detection of retinal layer structures on optical coherence tomography images. Optics Express Vol. 13(25), 10200-10216, Nov. 2005

[10] K.L. Boyer, A. Herzog et al.: Automatic Recovery of the Optic Nervehead Geometry in Optical Coherence Tomography. IEEE Transactions on Medical Imaging, Vol. 25(5), 553-570. May 2006